Surprising High Hydrophobicity of Polymer Networks from Hydrophilic Components

Agnese Attanasio,[†,‡] Ilker S. Bayer,*[‡] Roberta Ruffilli,[§] Farouk Ayadi,[†] and Athanassia Athanassiou*[‡]

[†]Smart Materials Platform, Center for Bio-Molecular Nanotechnologies@Unile, Istituto Italiano di Tecnologia (IIT), Via Barsanti, 73010 Arnesano (Lecce), Italy

[‡]Nanophysics Department, Istituto Italiano di Tecnologia (IIT), Via Morego, 16163 Genova, Italy

[§]Nanochemistry Department, Istituto Italiano di Tecnologia (IIT), Via Morego, 16163 Genova, Italy

Ⓢ *Supporting Information*
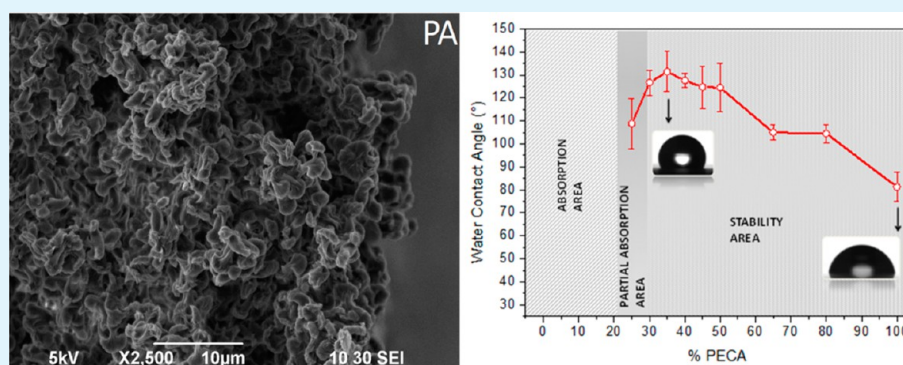
ABSTRACT: We report a simple and inexpensive method of fabricating highly hydrophobic novel materials based on interpenetrating networks of polyamide and poly(ethyl cyanoacrylate) hydrophilic components. The process is a single-step solution casting from a common solvent, formic acid, of polyamide and ethyl cyanoacrylate monomers. After casting and subsequent solvent evaporation, the in situ polymerization of ethyl cyanoacrylate monomer forms polyamide-poly(ethyl cyanoacrylate) interpenetrating network films. The interpenetrating networks demonstrate remarkable waterproof properties allowing wettability control by modulating the concentration of the components. In contrast, pure polyamide and poly(ethyl cyanoacrylate) films obtained from formic acid solutions are highly hygroscopic and hydrophilic, respectively. The polymerization of ethyl cyanoacrylate in the presence of polyamide promotes molecular interactions between the components, which reduce the available hydrophilic moieties and render the final material hydrophobic. The wettability, morphology, and thermo-physical properties of the polymeric coatings were characterized. The materials developed in this work take advantage of the properties of both polymers in a single blend and above all, due to their hydrophobic nature and minimal water uptake, can extend the application range of the individual polymers where water repellency is required.

KEYWORDS: polyamides, poly(ethyl-cyanoacrylates), interpenetrating polymer networks, wettability, hydrophobic surfaces

INTRODUCTION

The general aim for creating polymeric blends is to combine the properties of the respective components within a near homogeneous material, while overcoming some of their weaknesses, although the latter goal is not always reached.[1] Among other properties, control of wetting characteristics of polymer blends is becoming highly important due to their increasing use in various industries such as coatings, membranes, and biotechnology to name a few. Wetting of polymeric blends is a complex phenomenon and is strongly related to a number of parameters such as hydrophobicity or hydrophilicity of the blends' constituents, degree of phase separation, interfacial interactions, surface morphology, and chemical interactions.[2] Usually, blends of hydrophobic and hydrophilic polymers (such as copolymers) demonstrate intermediate wetting states depending on the relative constituent concentrations and degree of phase separation after forming.[3]

Polyamides or nylons (PA) are among the most widely used thermoplastics having applications in different industrial fields (textile industry, membrane fabrication, food packaging).[4−8] Polyamides consist of polyethylene segments $(CH_2)_n$ separated by recurring NH−CO (amide) groups. The latter units provide hydrogen bonds between adjacent chains giving unique properties (high crystalline structure, high melting point, mechanical robustness, and chemical stability).[5,9−11] However, they tend to absorb water far more than other conventional polymer resins due to the hydrophilic character of the amide

functionality.[12] Various efforts have been made for reducing polyamide's hygroscopic nature such as applying barrier coating layers, forming copolymers or blends, and use of nanofillers such as silica or clays for nanocomposite preparation.[4,13−17] Even if desired barrier properties could be obtained by multilayered films, for instance, the process generally requires use of nonbiodegradable materials and can be costly as well as may require presurface treatments and also adds to the thickness of the polyamide films.[4] Copolymers of polyamides generally display weaker barrier properties than pure polyamides,[4] and their wetting characteristics have not been reported in detail. To increase the surface hydrophobicity of polyamides, researchers incorporated fluoro-monomers on plasma pretreated polyamide by UV or thermally induced surface graft copolymerization; nevertheless, the reported enhancement in hydrophobicity was at a mediocre level.[13] A number of studies attempted to blend polyamides with hydrophobic polyolefins which need compatibilization by carboxyl group functionalization in order to establish interactions with the amine groups of polyamide.[14] The inorganic additives, such as silica nanoparticles, need to be functionalized with hydrophobic organic molecules in order to render the final nanocomposites hydrophobic.[16] Similarly, the most common polyamide nanoadditives, nanoclays, need to be functionalized properly to enhance water barrier properties.[17]

Cyanoacrylates, on the other hand, are commonly used as adhesives due to their strong bond forming ability with many types of different materials.[15,18] Moreover, novel application of cyanoacrylates are continuously appearing in the literature.[16−24] Their well-known biocompatibility and biodegradability have facilitated several medical or biological applications as well. They have bacteriostatic properties[19−21,25] and have been approved by the US Food and Drug Administration (FDA).[26] Cyanoacrylate monomers are highly susceptible to anionic polymerization, since an anionic species or a weak base such as water or amines can initiate their rapid polymerization.[15−19] Therefore, ambient humidity[16,20,21] and the presence of different types of amines[27] can start their polymerization easily. The mechanism is easy to initiate and can be rapidly implemented at room temperature.[19] In summary, the process involves initiator addition across the cyanoacrylate monomer double bond to produce a zwitterion, which subsequently reacts with the rest of the monomers to form the polymer.[27] So far, there exists a few studies of copolymers or blends based on cyanoacrylates;[28−33] the main challenge is attributed to their intrinsic poor processability related to their reactivity. Recently, it has been shown that certain solution processing ways can enable control over the degree of polymerization of cyanoacrylates allowing blending with other polymers in solution.[28] The main challenge of fabricating polymer blends and composites with cyanoacrylates is their high reactivity under ambient conditions as well as their instability under elevated temperatures.[29]

To the best of our knowledge, no reports exist on the preparation of polyamide cyanoacrylate blends in the form of interpenetrating polymer networks (IPNs) in the literature. An IPN, according to the IUPAC definition, is a polymer blend comprising two or more networks, which are at least partially interlaced on a molecular scale but not covalently bonded. A simple mixture of polymers is not an IPN.[1] In contrast to conventional polymer blends, IPNs exhibit a lower degree of phase separation and enhanced miscibility due to a particular entangled morphology resulting from the control of the preparation conditions.[34,35] In the present work, we demonstrate that ethyl cyanoacrylate (ECA) monomers and polyamide can form efficient IPNs resulting in unusual wetting and waterproof properties, much better than the individual polymers. The IPN coatings were obtained by a single-step solution casting process. Different blends were fabricated from formic acid dispersions of ECA and PA. Upon solvent evaporation, the low pH conditions due to formic acid disappears and ECA monomer starts cross-linking (a thermosetting process) forming the IPN (hereafter designated as PA-CA IPNs). Note that pure polymeric coatings obtained from separate formic acid solutions of PA and ECA were highly hygroscopic and hydrophilic, respectively. In contrast, PA-CA IPNs displayed unexpectedly high hydrophobicity due to mutual interactions taking place during the synthesis which prevent interaction of water with the hydrophilic amide functional groups on the surface.

EXPERIMENTAL SECTION

Materials. The chemicals used for the preparation of the PA-CA IPNs were polyamide 6.6 (PA 6.6) resin, ethyl cyanoacrylate (ECA) liquid monomer, and formic acid (FA). PA 6.6 pellets (molecular weight 120 000 with a degree of polymerization of 531; density 1.14 g/mL), ECA monomer (density 1.05 g/mL), and the solvent formic acid (purity ≥88.0%; density 1.22 g/mL at 25 °C) were all purchased from Sigma-Aldrich. All these chemicals were used as received, without further purification.

Methods. *Preparation of the Solutions.* PA 6.6 pellets were dissolved in FA to produce a 5% by weight polymer in solution. The dissolution of PA pellets in FA was carried out at room temperature without mechanical stirring, and it was completed in a few hours. The solutions were transparent and highly stable over long periods of time. Different amounts of liquid ECA monomers were added into the as prepared PA solution so that several ECA-PA dispersions could be prepared ranging from 0% (pure PA) up to 100% (pure ECA). In particular, apart from the pure compounds, the following combinations were prepared and tested (as weight percent of ECA monomer with respect the total amount of polymer in solution): 5%, 10%, 15%, 20%, 25%, 30%, 35%,40%, 45%, 50%, 65%, and 80%.

Preparation of the Films. Films were prepared by drop casting from solutions onto glass slides or silicon wafer substrates. Substrates were carefully washed before use with isopropanol and dried with nitrogen. The same amount of solution was deposited on each substrate, and the samples were left to dry slowly in a fume hood at room temperature. Note that carboxylic acids are inhibitors for cyanoacrylate polymerization so that no immediate polymerization of ECA monomer in the freshly deposited films was observed. Hence, FA has a double role in the process: it acts as a solvent for PA but also as a stabilizer for ECA monomers both in solution and during film formation. All the films were prepared at the same time and thus were subjected equally to ambient conditions of temperature and humidity.

Characterization of the Samples. Chemical Characterization: Fourier Transform Infrared Spectroscopy (FT-IR). To inspect the in situ polymerization of ECA monomer, the PA-CA coatings were analyzed by FT-IR measurements in the 4000−400 cm^{-1} spectral range (mid-IR region) using a VERTEX 70 FT-IR apparatus (absorbance mode at a resolution of 4 cm^{-1}). All the samples used were deposited by spin coating on a clean silicon wafer to avoid substrate interference signals.

Morphological Characterization: Scanning Electron Microscopy (SEM). To evaluate the morphological differences between the prepared PA-CA IPNs and to better follow the ECA polymerization progress, SEM micrographs were acquired using a JEOL JSM-6490LA. Both surface and cross sections of the coatings were inspected after being sputtered with 10 nm of carbon coating to reduce charging effects. In order to obtain cross section SEM images, the silicon substrate was cut perpendicularly to its surface by a simple cleavage fracturing. The strong adhesion of the films onto the substrate did not
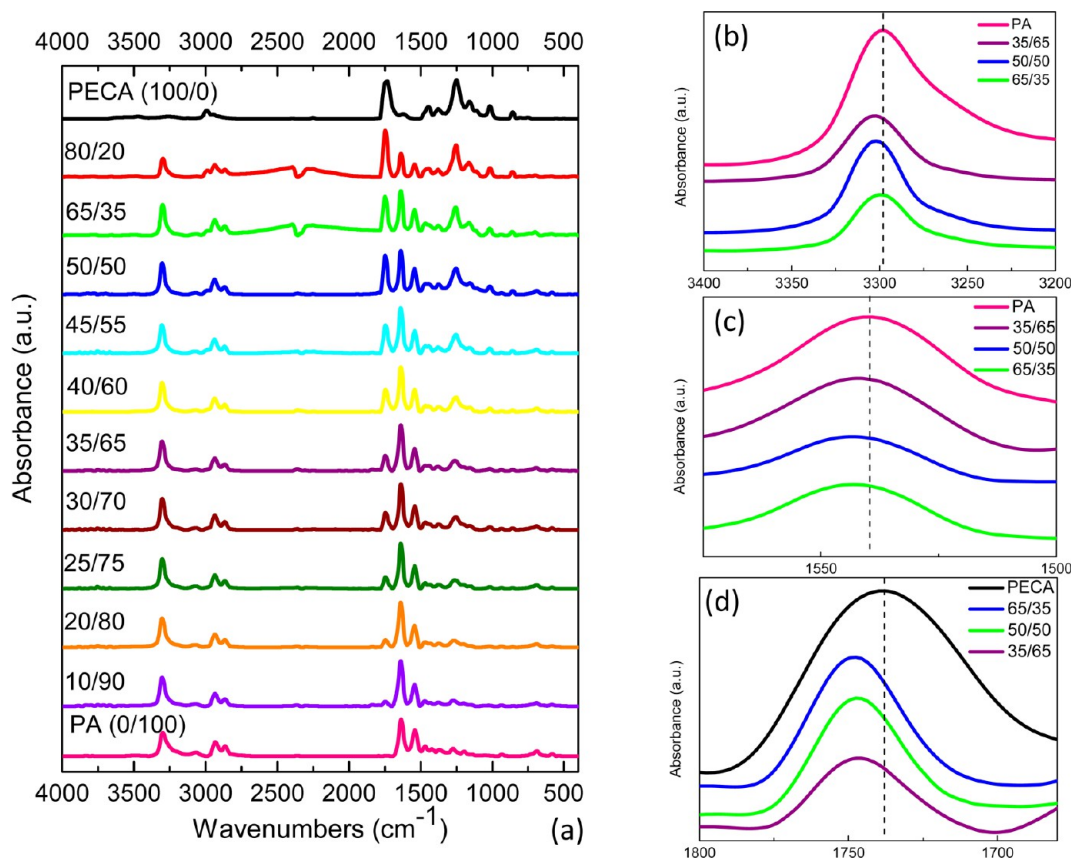
5718

dx.doi.org/10.1021/am401131u | ACS Appl. Mater. Interfaces 2013, 5, 5717−5726

Figure 1. Low resolution FTIR spectra (a) and magnification of the N−H stretching (b), N−H bending (c), and C=O stretching vibrations (d) of PA-CA IPNs in different ratios. The labels refer to PECA/PA (w/w) concentration within the IPNs.

give rise to any detachment between them, so the SEM imaging was performed without further treatments, apart from the carbon coating. The images of each sample were acquired by detecting the secondary electrons, which provided information about their morphology. The topographic images were recorded working in high vacuum and with an accelerating voltage of 5 kV. Every sample was imaged at different locations, and images of different magnification were collected. All the tested materials were deposited on clean silicon wafers.

Thermal Characterization: Thermogravimentric Analysis (TGA) and Differential Scanning Calorimetry (DSC) Measurements. Thermal analysis of pure materials and their blends was performed by thermogravimetric analysis (TGA) and differential scanning calorimetry (DSC) on a Mettler Toledo (TGA/DSC 1 Star System) instrument. Samples were scanned from 30 to 600 °C at a heating rate of 5 °C/min under nitrogen atmosphere set at a flow rate of 50 mL min^{-1}. TGA data were analyzed in the form of mass loss and rate of mass loss (first derivate of mass loss) with respect to the temperature. The materials degradation temperature was evaluated using TGA; in addition, crystal melting temperature and the corresponding heat of fusion (HOF) were obtained from the DSC signal. Moreover, the degree of crystallinity of the blends was calculated on the basis of the melting temperature of 100% crystalline PA 6.6 (HFO* = 190 J/g[36]) (see Supporting Information).

Water Contact Angle Measurements. The wetting behavior of the PA-CA IPNs was studied by measuring static and dynamic water contact angles (WCA) using the sessile water drop method. Measurements were performed on a KSV-CAM200 contact angle goniometer under ambient conditions. Distilled water was used as probe liquid and was dispensed using a microsyringe; the typical water drop volume was ~1 μL. For each sample, the static contact angle value was obtained from an average of six measurements recorded on different areas of the same surface avoiding the sample's edges. Change in droplet volume and apparent contact angle during absorption were

also recorded for 1 s and 1 min using the same goniometer in a transient mode using a CCD camera (see Supporting Information).

Water Uptake Measurements. Water uptake measurements were also carried out in order to find a possible correlation between the relative concentrations of the polymers and the amount of absorbed water. The following approach was used: dry samples were weighed on a sensitive electronic balance and then were totally covered with distilled water either for 1 min or for 24 h. Excess water accumulation on the surface of the samples was carefully removed by absorbing it with the corner of a lab tissue. The samples were then weighted again. Water uptake was evaluated as the absorbed water content relative to the original dry weight and was estimated using the following equation:

$$\text{WU (\%)} = \frac{W_{\text{f}} - W_{\text{i}}}{W_{\text{i}}} \times 100 \tag{1}$$

where W_{i} and W_{f} are the samples' weights in grams before and after water immersion, respectively.

■ RESULTS AND DISCUSSION

FTIR Analysis. FTIR spectra of PA, PECA (control experiments), and their PA-CA IPNs are presented in Figure 1a. The recorded data were used to investigate the ECA monomer conversion into PECA polymer and the possible interactions between PECA and PA during this process.

The major PECA absorption bands are similar to the typical spectra reported in other studies.[37−39] The examination of the two functional peaks, typically associated with the ECA monomer, shows that the one around 1615 cm^{-1} (C=C stretching)[37,40] has very low intensity, whereas the one at 3130 cm^{-1}, from =C−H stretching of vinyl structures (=CH$_2$, =CH−),[37,38] is absent, indicating that complete ECA monomer
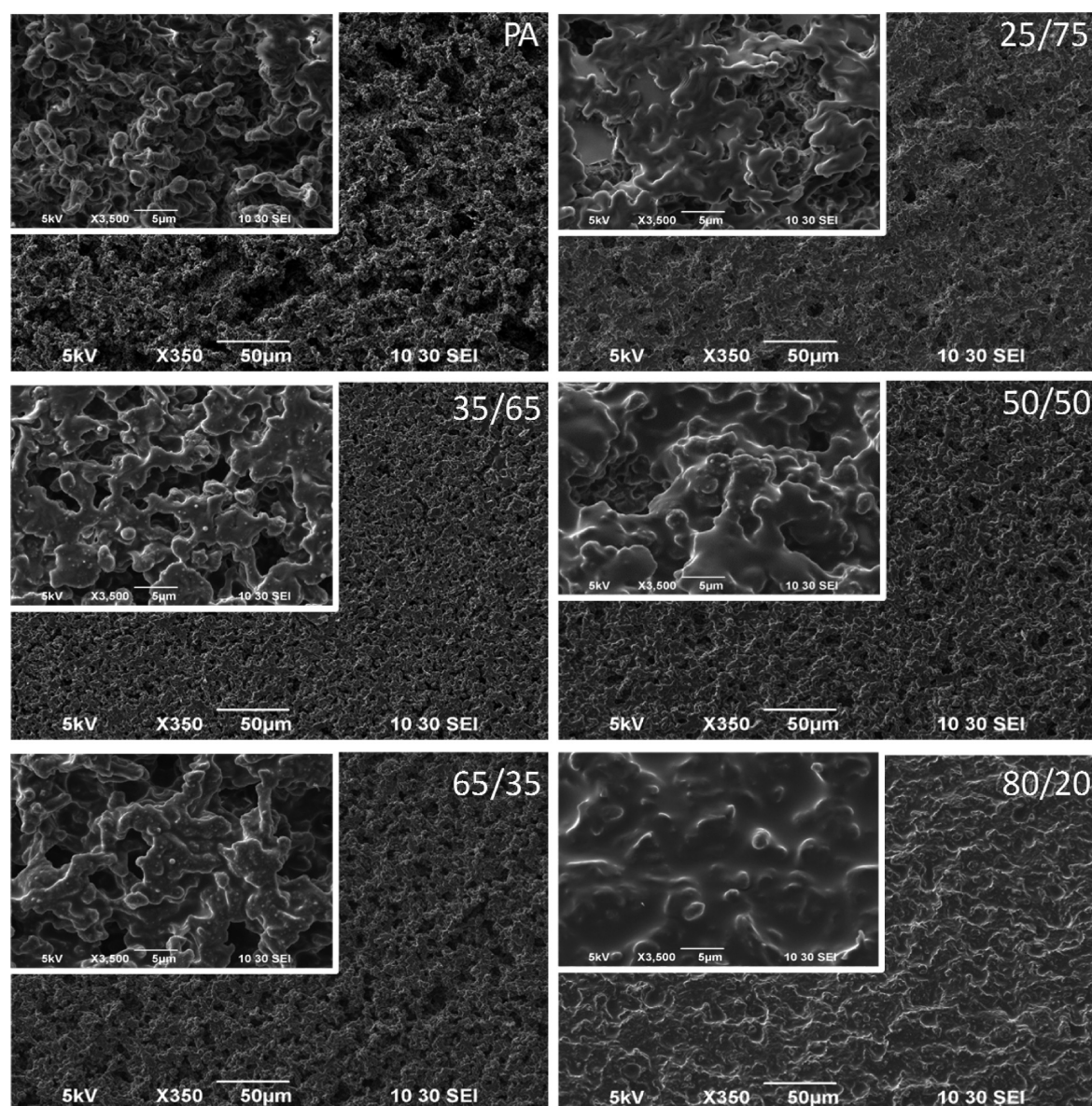
Figure 2. SEM micrographs of the top surface of pure PA porous samples and PA-CA IPNs with different relative ratios of the individual polymers, as produced by drop casting from formic acid solutions. The inset pictures show higher magnifications. The labels refer to PECA/PA (w/w) concentration into the IPNs.

polymerization was achieved. Interestingly, no evidence of unreacted monomers was detected in all the blends indicating that PA chains have no PECA polymerization hindering effect. The multiple broad peak between 3040 and 2860 cm^{-1} is due to the C–H stretching vibrations (symmetric and asymmetric) of the $-CH_2-$ and $-CH_3$ groups.[37] The prominent peak around 1750 cm^{-1} corresponds to the $-C≡O$ stretching vibration.[37,39,40] Moreover, the strong peak around 1254 cm^{-1} is ascribed to C–O–C asymmetric and symmetric stretches.[39]

The spectrum corresponding to pure PA also confirms data reported in earlier studies.[7,9,40,41] The strong peak around 3300 cm^{-1}, which is assigned to hydrogen-bonded N–H stretching,[9] can be observed, and also peaks at 2940 cm^{-1} (asymmetric CH_2 stretching) and 2876 cm^{-1} (symmetric CH_2 stretching)[7,9] are easily distinguished. The band corresponding to N–H bending[7,9,40,41] appears at 1534 cm^{-1}. The spectrum shows a strong band around 1632 cm^{-1} corresponding to C≡O (carbonyl group) stretching.[7,40,41]

FTIR analysis of PA-CA IPNs indicates that the intensity of the characteristic peaks ascribed to PECA gradually increase as the concentration of ECA in the solutions is increased from 10% up to 80%, therefore supporting the continuous change in the final film compositions. The results clearly show that there was no new peak formation, indicating that there is no formation of new phases. Since no new phase formation has been found, it can be assumed that no strong chemical interactions occur between the constituent polymers, which form a physical blend. As mentioned earlier, IPNs are a special case of polymer blends held together by mutual and forced chain entanglements. This can be obtained when one polymer network is formed in the immediate presence of the other. In this way, the reacting elements are blended thoroughly during synthesis showing a lower degree of phase separation in comparison to conventional blends.[42,43]

Magnified areas of the FTIR spectra from the N–H stretching (~3300 cm^{-1}) and bending (~1530 cm^{-1}) (peaks
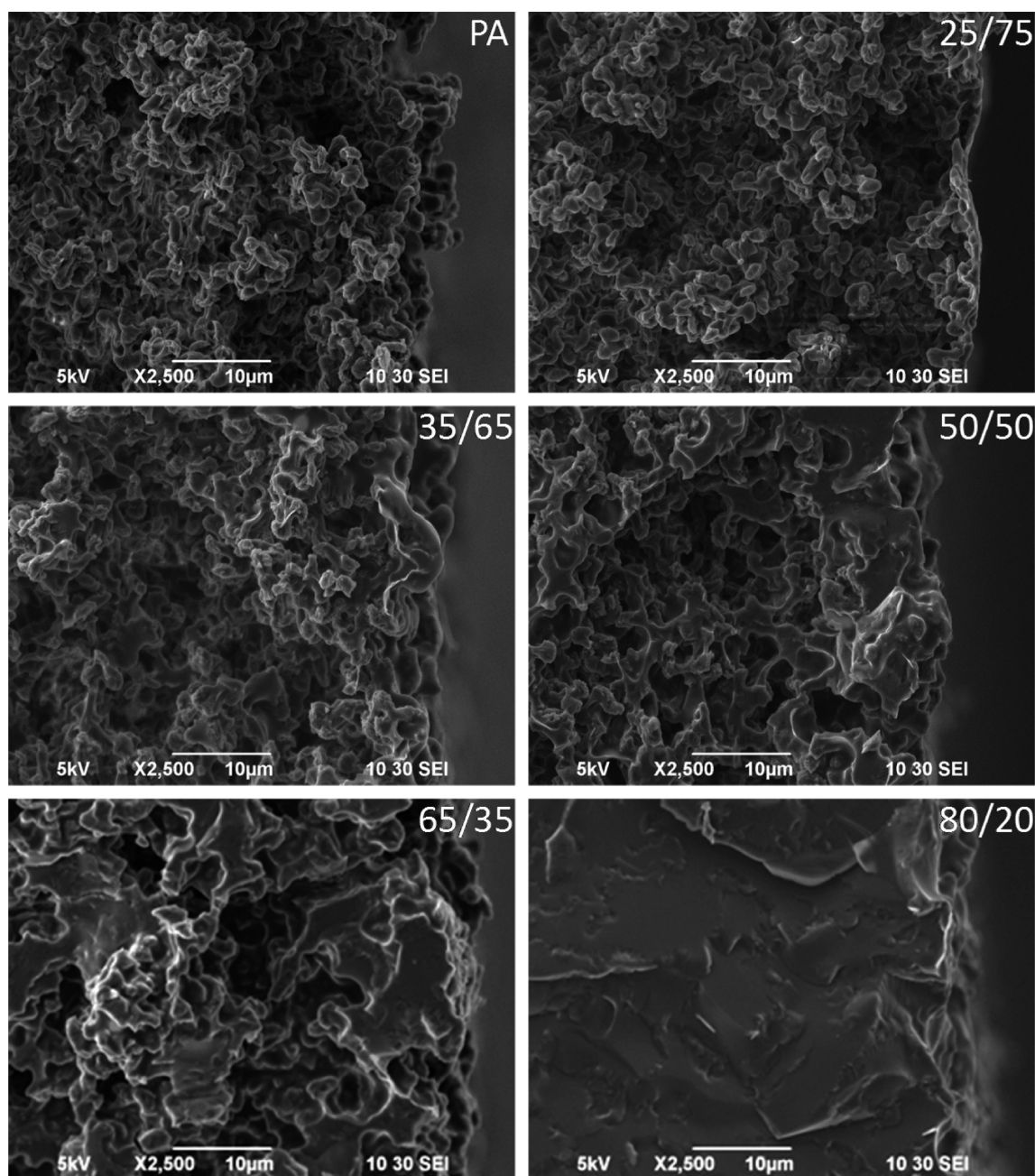
Figure 3. SEM micrographs of cross sections of pure PA and PA-CA IPNs at different relative ratios, as produced by drop casting from formic acid solutions. The labels refer to PECA/PA (w/w) concentration into the IPNs.

related to PA) and of the C═O stretching (∼1750 cm^{-1}) (peak related to PECA) at different PECA/PA ratios are displayed in Figure 1b–d, respectively. A small shift toward longer wavelengths in the amide and in the carbonyl signals of the blends is evident compared to the neat polymers. This shift suggests possible interactions between PA chains and the acrylic polymer. Therefore, we assume that hydrogen interactions in the blend between carbonyl groups of PECA and amidic groups of PA can readily occur[28,44] and may also help the compatibility and miscibility between PA and PECA of the IPN blends.

Surface Morphology Analysis. The morphology of the PA-CA polymers was inspected by SEM (top surface and cross section). As shown in Figure 2, pure PA casted from formic acid solutions and dried at ambient temperature has a porous

morphology resembling typical features of polyamide membranes.[16,45] Generally, nonporous polyamide films are hydrophilic, but porous polyamide is hygroscopic since it absorbs water. On the other hand, the morphology of pure PECA (not shown here), obtained by drop casting from formic acid solutions, appeared featureless and was homogeneous with amorphous nature. Figure 2 shows also SEM images of PA-CA IPN coatings with increasing PECA concentrations ranging from 25% to 80% by weight. The presence of PECA has an obvious influence on the morphology of the composite surfaces. In particular, IPNs with increasing PECA concentration show gradually reduced porosity and less irregular structures with respect to PA films, with a more evident interconnected network. From the magnified images, it can be seen that PECA polymer progressively covers the pores and
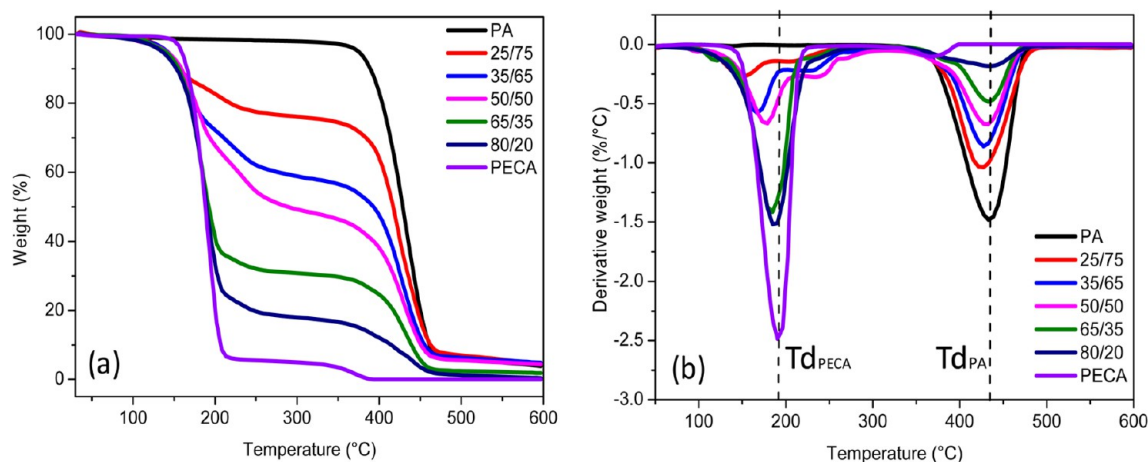
Figure 4. TGA curves of the neat PA and PECA polymers and PA-CA blends (a) and the first derivative of TGA (DTG) curves (b). The legend indicates different PECA/PA compositions in the IPNs.

features originating from PA surface as its concentration increases, resulting in a compact surface for the IPNs with 80 wt % PECA concentration.

It is worth noticing that as the concentration of the PECA in the blends reaches 35% by weight some new topological features appear as seen in the magnified SEM insets in Figure 2. These images indicate formation of submicrometer particle-like bumps within the blends. Such characteristic submicrometer particles are absent in pure PA and in the IPN surfaces containing lower PECA amounts. It is argued that they can be independent PECA domains formed on the surfaces, which do not interact with the PA polymer. For further details, see also Figure 1S (Supporting Information).

SEM investigation of the cross section of the samples was also conducted. In Figure 3, SEM images of pure polyamide and IPN blends with increasing PECA concentration are presented. PA presents porous domains similar to the structures seen on its surface throughout the entire thickness. This morphology does not seem to change considerably until 35 wt % PECA concentration above which PECA zones infused into the PA porous network are also seen. Notice that, at lower ECA concentrations, its polymerization is initiated preferably at the surface, where the polymerization can be largely activated by the environmental humidity and partially from the amide groups of the PA, and continues progressively toward the bulk.

TGA-DSC Studies. The thermal degradation behavior of the individual polymers (PA and PECA) and their IPNs is shown in Figure 4a. As already is known from the literature,[40,41] polyamides have excellent thermal stability compared to many acrylic polymers. The PA degradation takes place over a relatively narrow temperature range between 350 and 500 °C with the DTG peak (first derivate of TGA) for maximum weight loss occurring at 430 °C (see Figure 4b). These values are in agreement with previous reports on nylon's 6.6 thermal degradation.[41] The degradation of PECA takes place over a temperature range between 130 and 230 °C. The maximum rate of weight loss was found to be occurring at 190 °C from the DTG thermogram, as shown in Figure 4b. The relatively weak second inflection point at ~370 °C corresponds to the subsequent fragmentation of the suboligomeric chains formed in the previous degradation. Other researchers[40] have found that PECA degradation starts at about 160 °C, showing a maximum degradation at about 265 °C and complete degradation at around 300 °C. It has been suggested that

generally the thermal stability of such polymers depends on the nature of the initiator, polymerization conditions, and chains length.[29,40] It has been also shown that the polymerization rate of cyanoacrylates is lower in low pH environments so that their molecular weights are low.[46] In our experiments, during formic acid evaporation, a low pH environment is established within the cast films. This can interfere with the final polymeric molecular weight of PECA and therefore its degradation.

Thermal degradation of the PA-CA IPNs was found to be more intricate compared to those of pure polymers. The thermal decomposition peaks of the blends are not simple superposition of the degradation peaks of the individual polymer components but most likely are affected by the interactions occurring between the latter during in situ polymerization of ECA in the presence of PA. At least three inflection points were observed for all the IPNs as seen in Figure 4b. Two of them are related to PECA degradation and the third to PA degradation. Compared to pure PECA, the first peak for all the IPNs is progressively shifted toward lower degradation temperatures increasing the PA amount. This behavior could result from an effect of PA presence in the PECA polymerization mechanism. The two degradation steps related to PECA hint at different ways of PECA formation, resulting in different degrees of polymerization. Polymerization of ECA initiated by environmental moisture is expected to be rapid and produce a full-strength super glue-like polymer, whereas ECA polymerization initiated by amide groups present in PA can result at a different degree of polymerization, possibly showing a different degradation temperature. The third thermal degradation step associated with the PA component is also slightly modified with respect to pure PA indicating possible PA–PECA interactions within the IPNs. Careful inspection of the PA-related peaks in Figure 4b indicates that the maximum weight loss of PA-related species within the IPNs containing 25, 35, and 50 wt % PECA occurs at temperatures lower than those of pure PA. In contrast, the maximum weight loss of the PA-related species in the IPNs containing 65 and 80 wt % PECA occurs at temperatures similar to those of the neat PA. Therefore, we can assume that when the PECA concentration in the IPNs is lower than 50 wt % more interactions occur between the constituents than when PECA concentration exceeds that of PA, since in the latter case, the polymerization of ECA due to humidity seems to prevail. All the interactions described above between PA and PECA also influence the glass
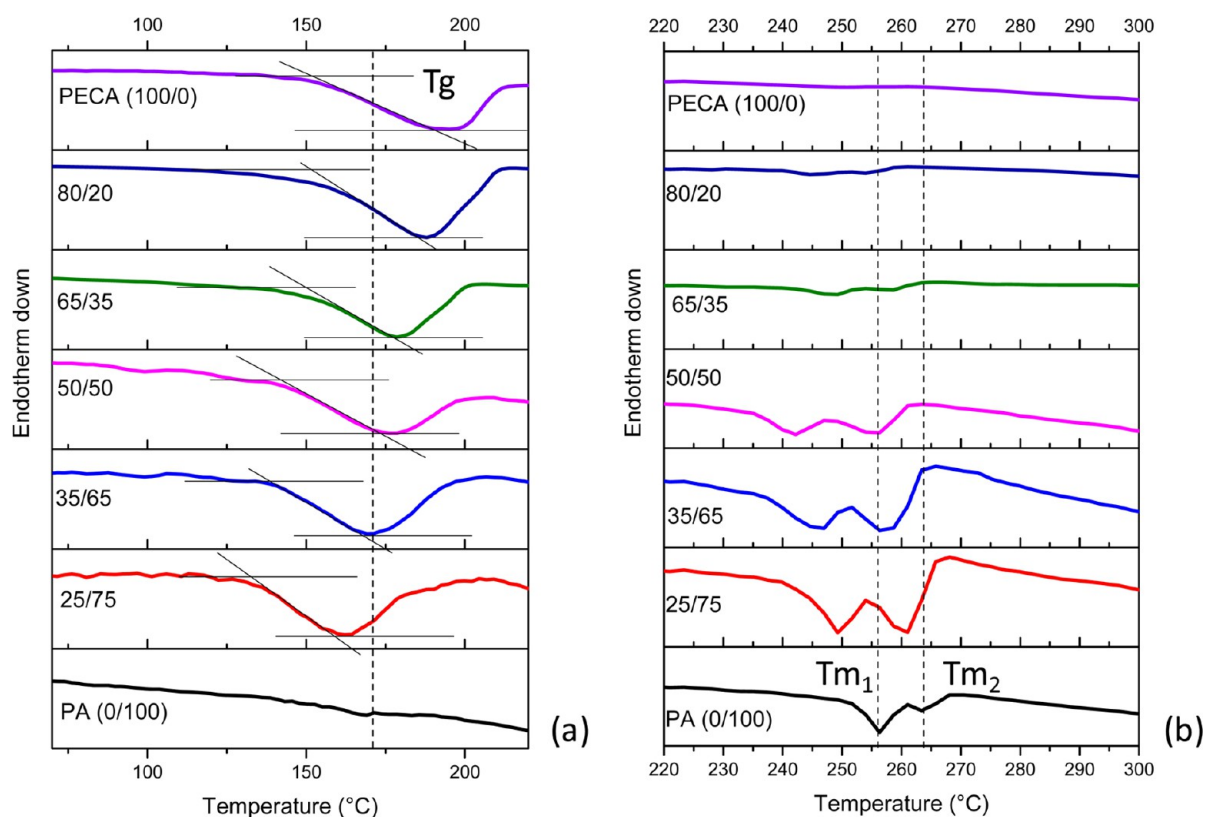
Figure 5. DSC curves at 5 °C/min of the neat polymers and PA-CA blends in different PECA/PA concentrations representing the T_g (a) and the T_{m_1} and T_{m_2} (b) shifts due to formation of the IPNs.

transition temperature (T_g) of PECA and the melting temperature of PA as shown in the DSC data in Figure 5b (for detailed discussion, see Table 1 in the Supporting Information). The IPNs display lower glass transition temperatures compared to pure PECA. The glass transition temperature of PA is around 50 °C (not detectable in these spectra due to the sensitivity of the instrument used). It appears that T_g of the IPNs is closer to pure PECA, although reduced, and no additional T_g appears. Full polymer miscibility is characterized by a single T_g in the blends, whereas in compatible blends two T_g values are measured. Hence, these IPNs can be characterized as a fully miscible polymer network.

Wettability of the IPNs. Figure 6 shows the static water contact angle measurements as a function of PECA inclusion in the blends. It is interesting to note that, depending on the relative weight percent between PECA and PA distinct wetting, regimes emerge. Namely, three different wetting regions are apparent in the graph denoted as water absorption region (0−20 wt % PECA), partial water absorption region (21−29 wt % PECA), and stability region (30−100 wt % PECA).

In particular, pure PA samples are totally hygroscopic, absorbing the water droplets as soon as they are placed on their surfaces, allowing no water contact angle measurements, consistent with previous wetting experiments on porous polyamide films.[16] For IPN samples with PECA content up to approximately 20 wt %, similar wetting behavior was observed; specifically, the water droplets spread and got absorbed into the surface within few seconds after deposition. New wetting trends appear, however, when more of the PECA is incorporated. For instance, in the case of 25 wt % PECA, the water drops attain initially a partial wetting state on the samples with finite contact angles, but after some minutes, they get
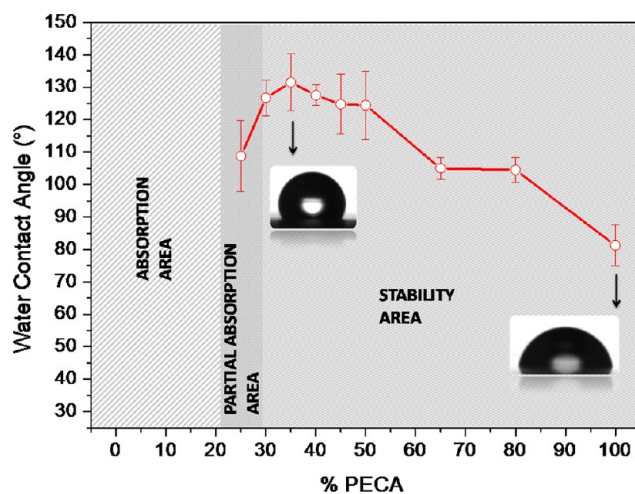

Figure 6. Static water contact angles and standard deviations for different PA-CA IPN blends with respect to PECA concentration. The insets show pictures of a ~1 μL water drop placed on the corresponding surfaces.

completely absorbed into the samples. During this metastable transitional stage, these initial static contact angles could be measured before complete absorption and are reported in Figure 6. Figure 2S in the Supporting Information demonstrates the dynamic changes in contact angles measured on IPN samples containing 25 and 30 wt % of PECA, for comparison purposes. Samples with 25 wt % PECA partially absorb water, whereas ones with 30 wt % PECA show no changes in contact angles and droplet volume over time, indicating that in order to obtain highly stable hydrophobic (≥125°) PA-CA IPNs a

5723

dx.doi.org/10.1021/am401131u | ACS Appl. Mater. Interfaces 2013, 5, 5717−5726
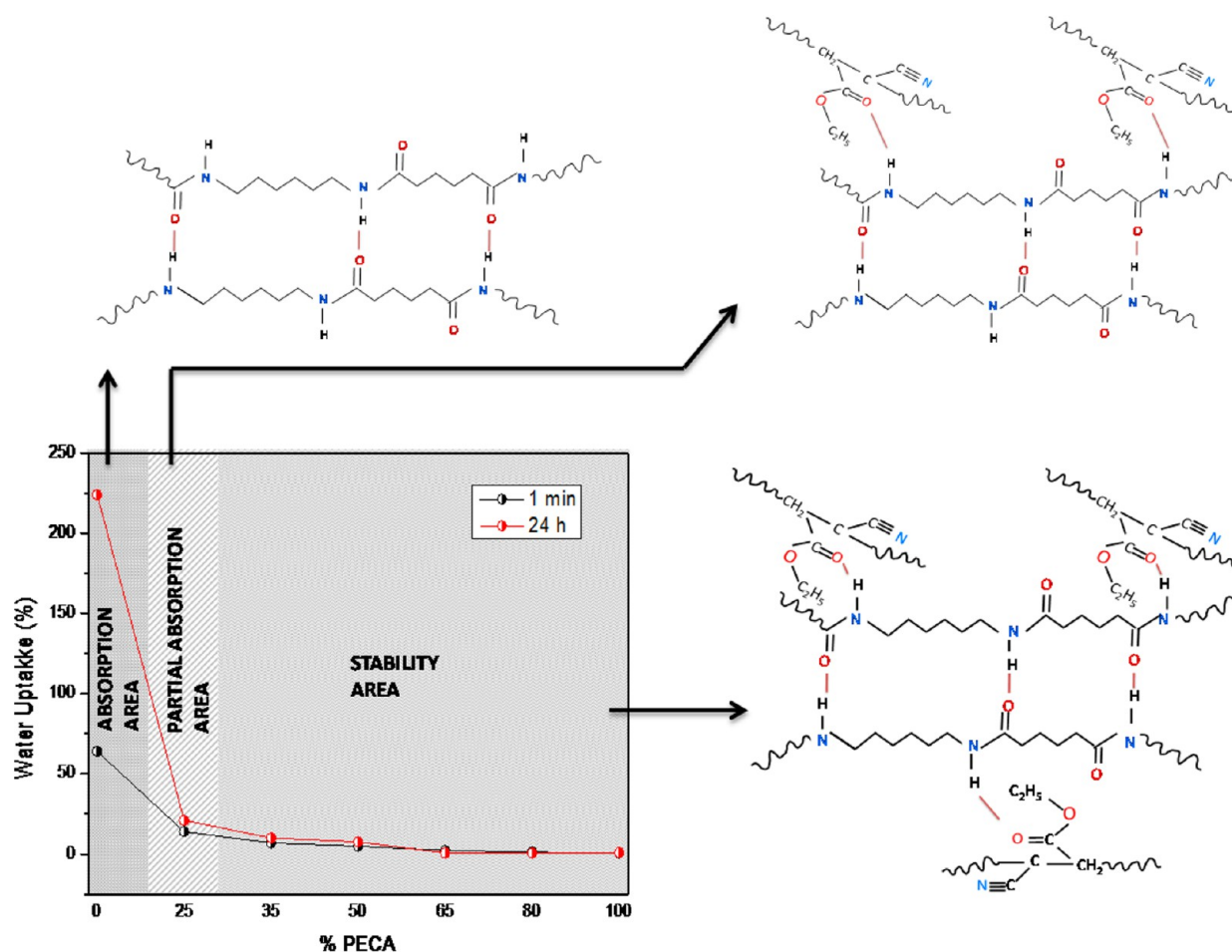
Figure 7. Percent water uptake from PA-CA IPN blends, showing the dramatic decrease of water content even at low PECA concentrations. PA molecular chains with nonbonded hydrophilic amide moieties and proposed hydrogen bonding interactions between the NH groups of PA and the C=O groups of PECA in the blends are also shown. These interactions prevent the material from external water, exposing more hydrophobic groups on the surface.

minimum amount of 30% wt PECA is required. The maximum contact angles values ($\sim$131.5 $\pm$ 8.7°) were reached at $\sim$35 wt % PECA concentration. Further increase in the PECA content up to 50 wt % causes a slight decrease in the water contact angle ($\sim$125°), and above that point, the decrease becomes bigger ($\sim$105° for the 65% and 80% samples) even if the material still remains hydrophobic. The reduction in the hydrophobicity of the IPNs above 35 wt % PECA might be the result of the excessive PECA formation on the surfaces. Control experiments on pure PECA were also performed and indicated stable WCAs at $\sim$81° confirming its hydrophilic character. This value was somewhat higher than other data reporting WCAs of 68°.[47] This difference could be due to the ECA polymerization history or/and due to the acid dissolution of ECA. In the present study, ECA polymerization is delayed due to the acidic solvent evaporation and disappearance of low pH environment, compared to other studies where sudden polymerization due to high humidity was realized. In summary, the WCA measurements revealed that the PA-CA IPNs demonstrate remarkable hydrophobic properties, if we consider that they are formed by the combination of highly water-absorbing (PA) and hydrophilic (PECA) individual constituents.

Figure 7 presents the results of water uptake for different PA-CA blends after the immersion in water either for 1 min or for 24 h. Results demonstrate significant decrease in water uptake

as the PECA content increases, indicating that ECA monomer-induced IPNs not only changes surface wettability but also limits the amount of water absorbed into the bulk of the materials. The highest water uptake, as expected, was observed for pure PA ($\sim$65% in 1 min and 225% after 24 h) whereas PECA does not absorb water ($\sim$0%). Up to 25% of PECA water uptake occurs upon immersion since, as shown in Figure 6, the materials at these compositions show partial water droplet absorption. The water absorption is definitely reduced in the stability area even if a very small amount of water can still penetrate the sample. Water uptake of a polymer is affected by the polymer's free volume and density, which depend on, among the other things, the fabrication technique.[48] The tested IPNs were deposited by solvent casting so that the resulting nondense morphology justifies some water uptake. As seen in Figure 7, while PA continues to absorb water with time, the PA-CA IPNs maintain a stable water absorption resistance even after 24 h.

Moreover, in Figure 7, we schematically demonstrate the proposed model showing hydrogen bonding interactions between the two polymers in the IPNs. We argue that the interactions between the amide groups of PA and the carbonyl group of PECA are responsible for the dramatic decrease in the water absorption and for the hydrophobic character of the IPNs. This claim seems to be supported by the FTIR and the

TGA/DSC measurements presented earlier. These bonds are formed during the spontaneous polymerization of ECA monomer once the common solvent is evaporated. In the blends, due to structural rearrangements, the amide functionalities are gradually covered by PECA, and in turn, the hygroscopicity was modified. The amide−carbonyl interactions, particularly on the surface of the materials, are expected to reduce the polar dangling amide groups at the solid−air interface, reducing their hydrophilic effects. At high PECA concentrations, the relative density of the carbonyl groups is also high with respect to the density of the available amide groups. Therefore, more carbonyl groups are available to interact with free amide groups, reducing the density of the latter further.

CONCLUSIONS

In this work, novel PA-CA IPNs based on polyamide (PA) and ethyl cyanoacrylate (ECA) monomers were successfully prepared by a one-step polymerization method by solvent casting from formic acid solutions. The IPNs were formed by in situ ECA polymerization once the acidic solvent evaporated. The anionic polymerization of the monomer was catalyzed by naturally occurring moisture and also with the presence of PA's amide groups. FTIR analysis confirmed formation of PECA in all the blends studied. Morphological observations revealed a good dispersion of the constituent polymers in the blends and that PECA gradually fills the porous structure of PA. Evidence of polymer interactions in the PA-CA IPNs was also confirmed by detailed chemical and thermal characterization experiments. PA and PECA can interact within the IPNs by forming hydrogen bonds between N−H groups of PA and C=O groups of PECA. These interactions were shown to render the IPNs hydrophobic and establish an inherent resistance to water penetration. At lower PECA concentrations (21−29 wt %), the IPNs showed some degree of resistance against water absorption but were not stable in time. IPNs with higher PECA inclusion became hydrophobic showing a maximum water contact angle of around 132° at 35 wt % in PECA concentration, which was stable in time. This simple and cost-effective technique is expected to expand the use of both PA and PECA in various applications, especially where high hydrophobicity is required including new generation food packaging and medical or biocompatible materials.

ASSOCIATED CONTENT

ⓢ Supporting Information

High magnification SEM images of the IPN films; glass transition and melting temperature results from differential scanning calorimetry measurements; dynamic water contact angle results from wetting of IPNs containing 25% and 30% PECA. This material is available free of charge via the Internet at http://pubs.acs.org.

AUTHOR INFORMATION

Corresponding Author

*E-mail: ilker.bayer@iit.it (I.S. Bayer); athanassia.athanassiou@iit.it (A. Athanassiou).

Notes

The authors declare no competing financial interest.

REFERENCES

(1) Chikh, L.; Delhorbe, V.; Fichet, O. *J. Membr. Sci.* **2011**, *368*, 1−17.
(2) Geoghegan, M.; Krausch, G. *Prog. Polym. Sci.* **2003**, *28* (2), 261−302.
(3) Meuler, J.; Nieves, A. R.; Mabry, J. M.; Cohen, R. E.; McKinley, G. H. *Soft Matter* **2011**, *7* (21), 10122−10134.
(4) Del Nobile, M. A.; Buonocore, G. G.; Palmieri, L.; Aldi, A.; Acierno, D. *J. Food Eng.* **2002**, *53*, 287−293.
(5) Zhang, J.; Khong, K. T.; Kang, E. T. *J. Appl. Polym. Sci.* **2000**, *78*, 1366−1373.
(6) Xu, F. J.; Zhao, J. P.; Kang, E. T.; Neoh, K. G.; Li, J. *Langmuir* **2007**, *23*, 8585−8592.
(7) Lim, L-T; Britt, I. J.; Tung, M. A. *J. Appl. Polym. Sci.* **1999**, *71*, 197−206.
(8) Gao, Z.; Sun, J.; Peng, S.; Yao, L.; Qiu, Y. *J. Appl. Polym. Sci.* **2011**, *120*, 2201−2206.
(9) Benhui, S. *Chin. J. Polym. Sci.* **1994**, *12*, 57−65.
(10) Dasgupta, S.; Hammond, W. B.; Goddard, W. A., III *J. Am. Chem. Soc.* **1996**, *118*, 12291−12301.
(11) Zhang, L.; Zhang, X.; Dai, Z.; Wu, J.; Zhao, N.; Xu, J. *J. Colloid Interface Sci.* **2010**, *345*, 116−119.
(12) Reuvers, N. J. W.; Huinink, H. P.; Fisher, H. R.; Adan, O. C. G. *Macromolecules* **2012**, *45*, 1937−1945.
(13) Zhang, J.; Khong, K. T.; Kang, E. T. *J. Appl. Polym. Sci.* **2000**, *78*, 1366−1373.
(14) Valenza, A.; Visco, A. M.; Acierno, D. *Polym. Test* **2002**, *21*, 101−109.
(15) Arora, A.; Padua, G. W. *J. Food Sci.* **2010**, *75*, R43−R49.
(16) Guo, Y.; Wang, Q.; Wang, T. *J. Mater. Sci.* **2011**, *46*, 4079−4084.
(17) Picard, E.; Gerard, J. F.; Espuche, E. *J. Membr. Sci.* **2008**, *313*, 284−295.
(18) Ng, C.-W. A.; Bellinger, M. A.; MacKnight, W. J. *Macromolecules* **1994**, *27*, 6942−6947.
(19) Walsh, D. J.; Rostami, S. *Ad. Polym. Sci.* **1985**, *70*, 119.
(20) Molnar, A.; Eisenberg, A. *Macromolecules* **1992**, *25*, 5774.
(21) Milliman, H. W.; Ishida, H.; Schiraldi, D. A. *Macromolecules* **2012**, *45* (11), 4650−4657.
(22) Bayer, I. S.; Fragouli, D.; Attanasio, A.; Sorce, B.; Bertoni, G.; Brescia, R.; Di Corato, R.; Pellegrino, T.; Kalyva, M.; Sabella, S.; Pompa, P. P.; Cingolani, R.; Athanassiou, A. *ACS Appl. Mater. Interfaces* **2011**, *3* (10), 4024−4031.
(23) Cingolani, R.; Athanassiou, A.; Pompa, P. P. *Nanomedicine* **2011**, *6* (9), 1493−1495.
(24) Ayadi, F.; Bayer, I. S.; Fragouli, D.; Liakos, I.; Cingolani, R.; Athanassiou, A. *Cellulose* **2013**, *20*, 1501−1509.
(25) Liu, Z.; Deng, Y.; Han, Y.; Chen, M.; Sun, S.; Cao, C.; Zhou, C.; Zhang, H. *Ind. Eng. Chem. Res.* **2012**, *51*, 9235−9240.
(26) Chiu, F. C.; Lai, S. M.; Chen, Y. L.; Lee, T. H. *Polymer* **2005**, *46*, 11600.
(27) Hemlata, S.; Maiti, N. *J. Polym. Res.* **2012**, *19*, 9926.
(28) Tiwari, M. K.; Bayer, I. S.; Jursich, G. M.; Schutzius, T. M.; Megaridis, C. M. *Macromol. Mater. Eng.* **2009**, *294*, 775−780.
(29) Han, M. G.; Kim, S. *Polymer* **2009**, *50*, 1270−1280.
(30) Tiwari, M. K.; Bayer, I. S.; Jursich, G. M.; Schutzius, T. M.; Megaridis, C. M. *ACS Appl. Mater. Interfaces* **2010**, *2*, 1114−1119.
(31) Bayer, I. S.; Tiwari, M. K.; Megaridis, C. M. *Appl. Phys. Lett.* **2008**, *93*, 173902−173905.
(32) Borgini, T.; Carpaneto, L.; Costa, G.; Stagnaro, P.; Valenti, B. *Mol. Cryst. Liq. Cryst. Sci. Technol. Sect. A. Mol. Cryst. Liq. Cryst.* **1999**, *336*, 199−210.
(33) Ivanova, M. P.; Kotzev, D. L. *Eur. Polym. J.* **1990**, *26*, 189−190.
(34) Widmaier, J.-M.; Chenal, J.-M. *Macromol. Symp.* **2004**, *216*, 179−187.
(35) Merlin, D. L.; Sivasankar, B. *Eur. Polym. J.* **2009**, *45*, 165−170.
(36) Sengupta, R.; Bandyopadhyay, A.; Sabharwal, S.; Chaki, T. K.; Bhowmick, A. K. *Polymer* **2005**, *46*, 3343−3354.

(37) Tomlinson, S. K.; Ghita, O. R.; Hooper, R. M.; Evans, K. E. *Vib. Spectrosc.* **2006**, *40*, 133−141.

(38) Zhou, Y.; Bei, F.; Ji, H.; Yang, X.; Lu, L.; Wang, X. *J. Mol. Struct.* **2005**, *737*, 117−123.

(39) Georgi, Y. *Cent. Eur. J. Chem.* **2012**, *10* (2), 305−312.

(40) Khalid, M.; Mohammad, F. *eXPRESS Polym. Lett.* **2007**, *1* (11), 711−716.

(41) Liu, W.; Zhang, S.; Chen, X.; Yu, L.; Zhu, X.; Feng, Q. *Polym. Degrad. Stab.* **2010**, *95*, 1842−1848.

(42) Hillerstrom, A.; Andersson, M.; Pedersen, J. S.; Altskar, A.; Langton, M.; Stam, J.; Kronberg, B. *J. Appl. Polym. Sci.* **2009**, *114*, 1828−1839.

(43) Kim, S. J.; Lee, K. J.; Lee, S. M.; Kim, I. Y.; Lee, Y. M.; Kim, S. I. *J. Appl. Polym. Sci.* **2003**, *88*, 2570−2574.

(44) Carone, E.; Felisberti, M. I. *J. Mater. Sci.* **1998**, *33*, 3729−3735.

(45) Lin, D.-J.; Chang, C.-L.; Lee, C.-K.; Cheng, L.-P. *Eur. Polym. J.* **2006**, *42*, 356−367.

(46) Katti, D.; Krishnamurti, N. *J. Appl. Polym. Sci.* **1999**, *74*, 336−344.

(47) Cai, B.-X. *J. Appl. Polym. Sci.* **2004**, *92*, 1005−1010.

(48) Valenzuela, L. M.; Michniak, B.; Kohn, J. *J. Appl. Polym. Sci.* **2011**, *121*, 1311−1320.